LIÈGE université

von KARMAN INSTITUTE FOR FLUID DYNAMICS

Development of a 3D time accurate HDG solver for ICP

ACOMEN 2022.

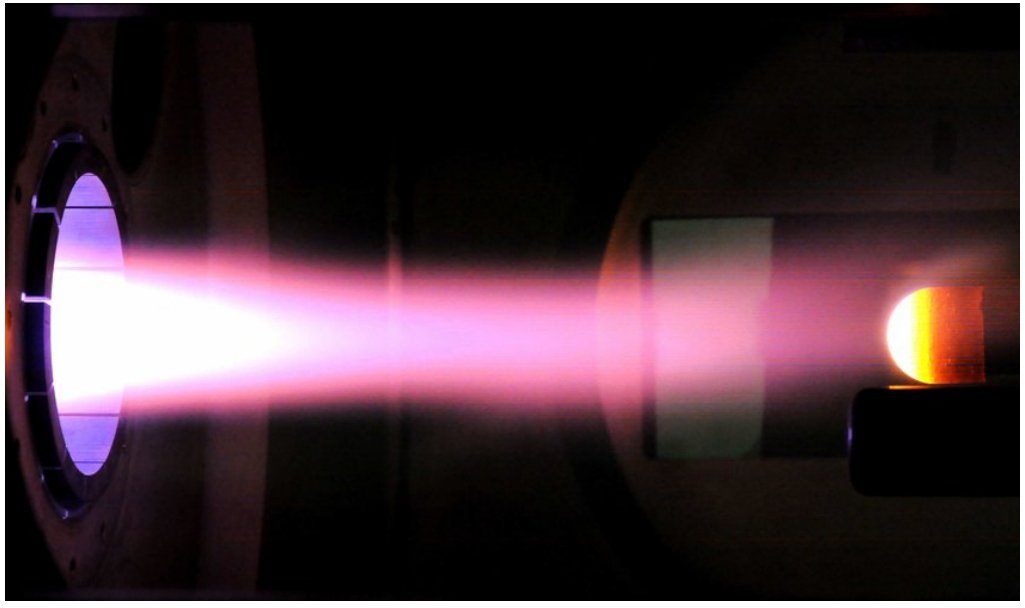

Author: Corthouts Nicolas

Promoters: Hillewaert Koen, May Georg

What is an inductively coupled plasma (ICP)?

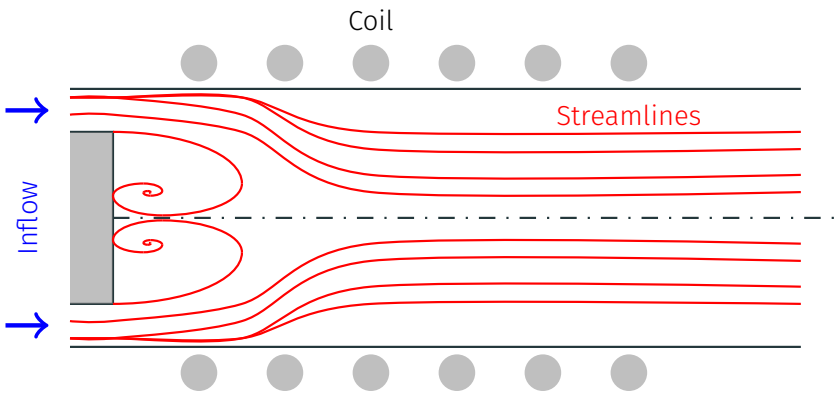

Torch

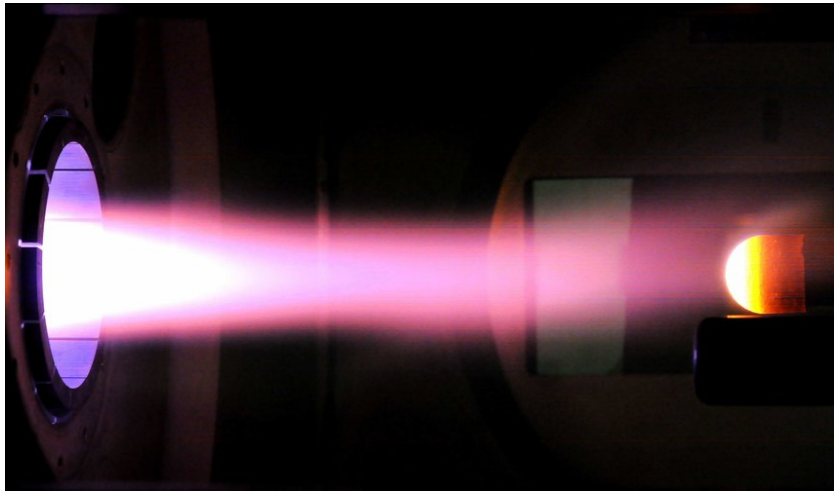

Test chamber

The most powerful ICP facility in the world, the Plasmatron, is located at VKI.

N.B. The governing equations are Maxwell + Navier-Stokes.

What is ICP purpose?

Demise of space debris

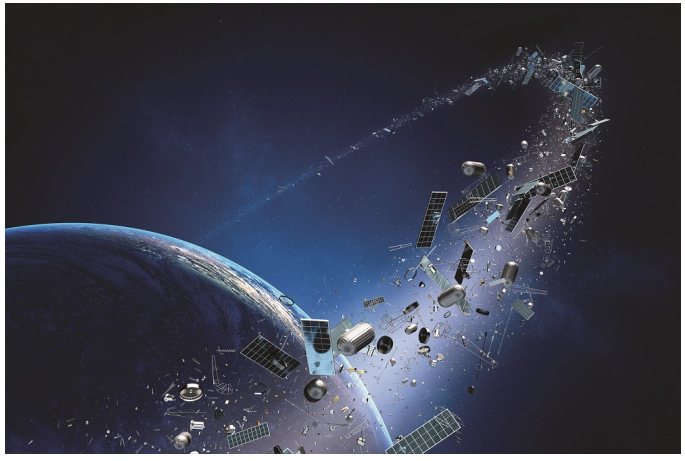

Thermal protection

The Plasmatron is involved in ESA projects. Having a reliable numerical solver for ICP is of great importance.

The problem with current ICP simulations

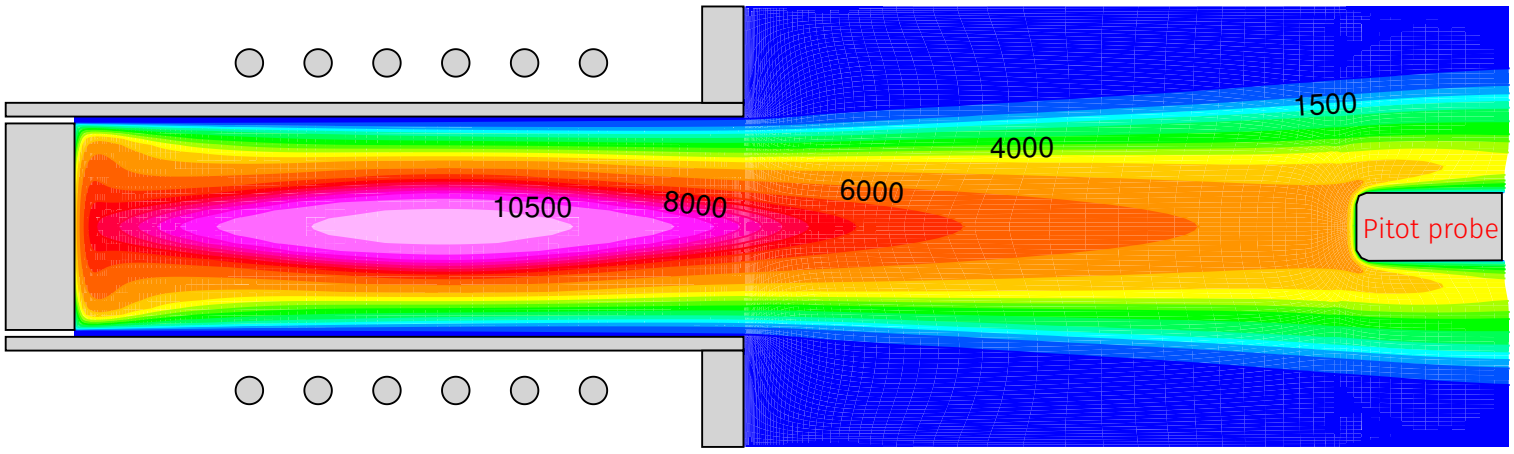

- **Usually FV** $\Longrightarrow$ hard to capture high spatial frequencies. X
- **Usually not 3D** $\Longrightarrow$ no 3D effects. X
- **Usually not time-accurate** $\Longrightarrow$ no unsteadiness. X

Need of a 3D, high-order time-accurate solver for ICP!

The numerical method: HDG

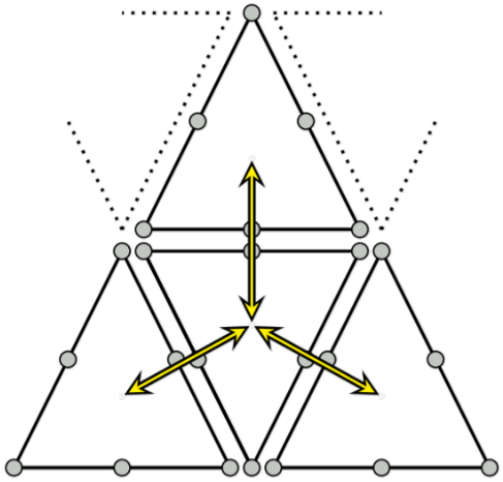

Classic DG.

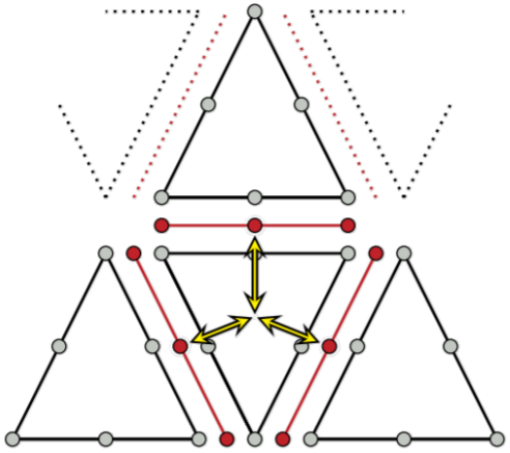

HDG: traces.

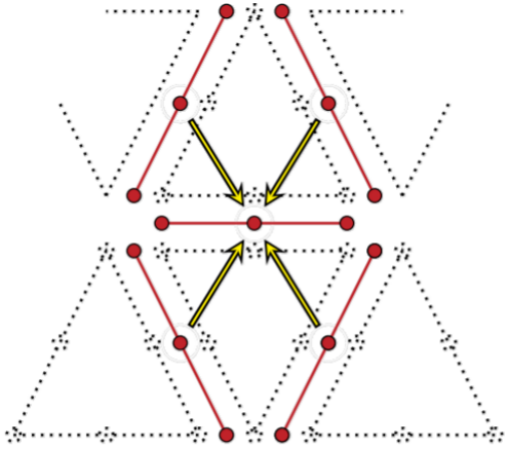

HDG: elements as transmitters.

This method requires solving 2 types of systems:

1. **Local systems** solved directly & in parallel.
2. **A global system** smaller than the global DG system. Can also be run in parallel.

The numerical method: HDG

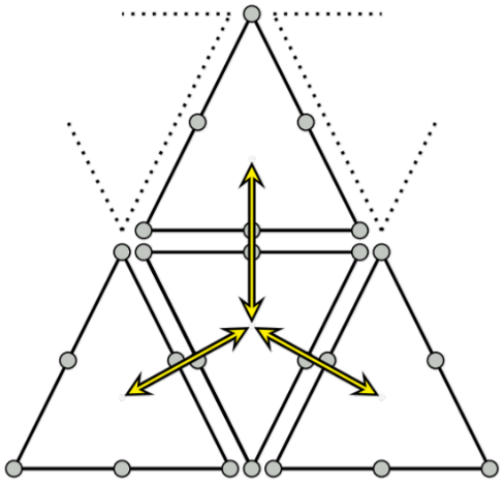

Classic DG.

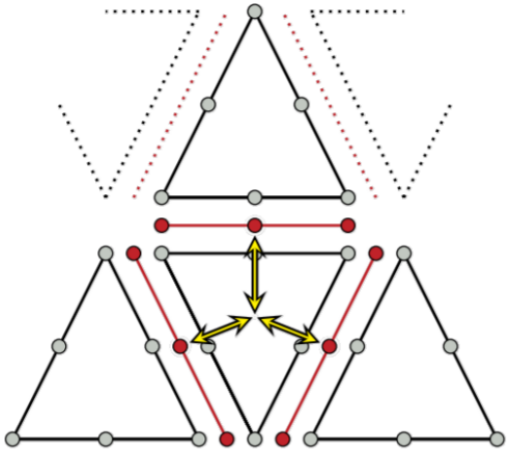

HDG: traces.

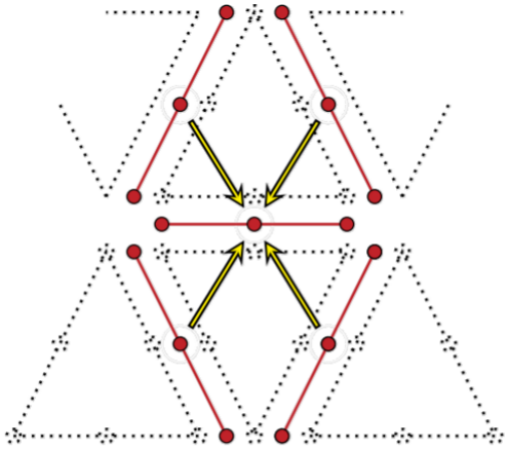

HDG: elements as transmitters.

The code (**Unified Framework**) used has been developed by the group of Prof. May.

Chemistry: Mutation++

Ideal gas description is not sufficient anymore. Complex chemistry is at play.

For now, the mixture is at **local thermodynamic equilibrium**!

Computational considerations: primitive variables

Observation: Mutation++ at LTE is much faster in finding the equilibrium for given p, T than with ρ and ρe.

1. implement the change of variables $\rho,\ \rho u, \rho e \rightarrow p,\ u\ T$.
2. ... such that it is general enough to be reused in the code easily.

Computational considerations: primitive variables

Observation: Mutation++ at LTE is much faster in finding the equilibrium for given p, T than with ρ and ρe.

1. implement the change of variables $\rho,\ \rho u, \rho e \rightarrow p,\ u\ T$.
2. ... such that it is general enough to be reused in the code easily.

General philosophy: keep the conservative form, but evaluate using the primitive variables only.

Computational considerations: primitive variables

Observation: Mutation++ at LTE is much faster in finding the equilibrium for given p, T than with ρ and ρe.

1. implement the change of variables $\rho,\ \rho u, \rho e \to p,\ u\ T$.
2. ... such that it is general enough to be reused in the code easily.

General philosophy: keep the conservative form, but evaluate using the primitive variables only.

Ex: We consider the change of variable from $u \to \lambda$.

$$\partial_t u + \nabla \cdot F_c(u) - \nabla \cdot F_v(u, \nabla u) = S(u, \nabla u)$$

Computational considerations: primitive variables

Observation: Mutation++ at LTE is much faster in finding the equilibrium for given p, T than with ρ and ρe.

1. implement the change of variables $\rho,\ \rho u, \rho e \rightarrow p,\ u\ T$.
2. ... such that it is general enough to be reused in the code easily.

General philosophy: keep the conservative form, but evaluate using the primitive variables only.

Ex: We consider the change of variable from $u \rightarrow \lambda$.

$$\partial_t u(\lambda) + \nabla \cdot F_c(\lambda) - \nabla \cdot F_v(\lambda, \nabla\lambda) = S(\lambda, \nabla\lambda)$$

Computational considerations: (very) low Mach

In high enthalpy flows, the **Mach can be very low**.

Computational considerations: (very) low Mach

In high enthalpy flows, the **Mach can be very low**.

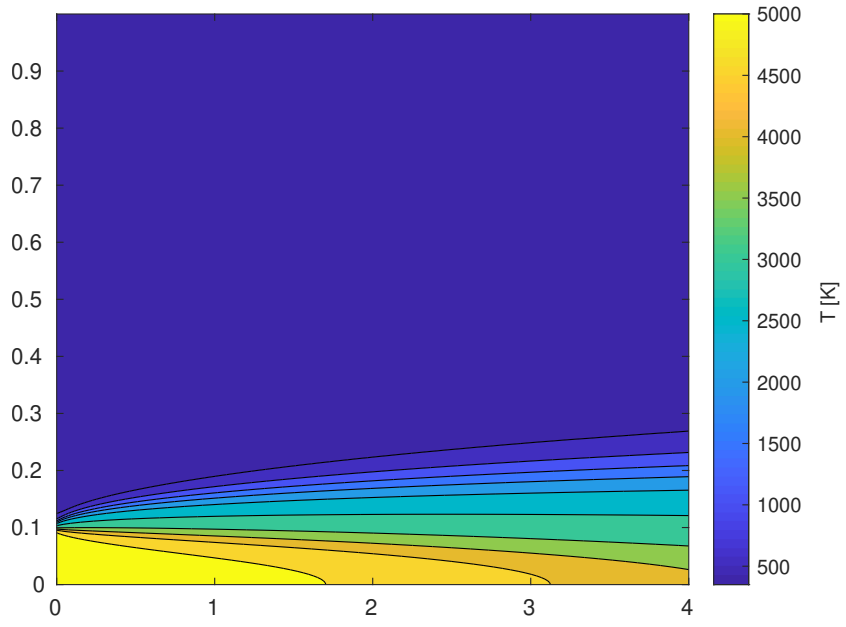

Computational considerations: (very) low Mach

In high enthalpy flows, the **Mach can be very low**.

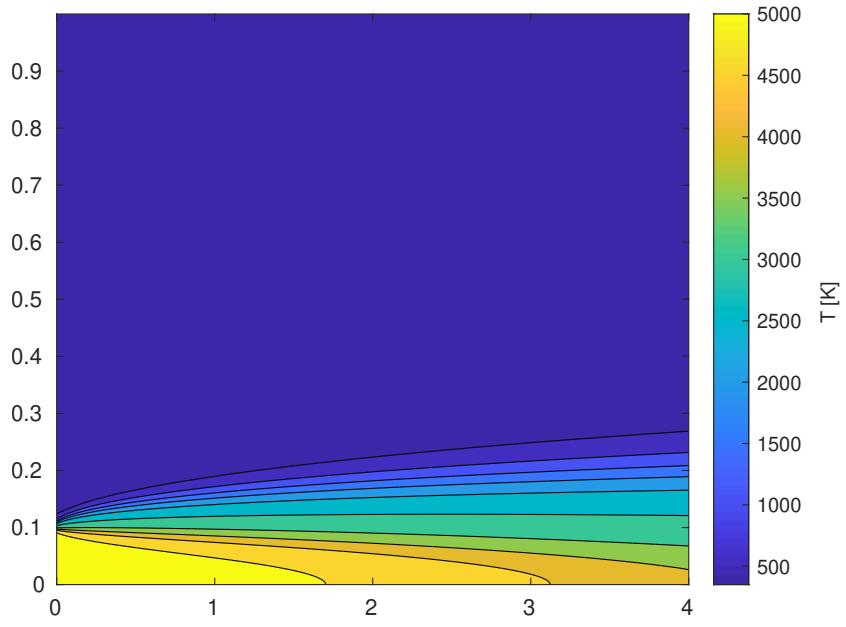

With U = 58.5 m/s at the centerline, Ma = 0.037

Computational considerations: (very) low Mach

In high enthalpy flows, the **Mach can be very low**.

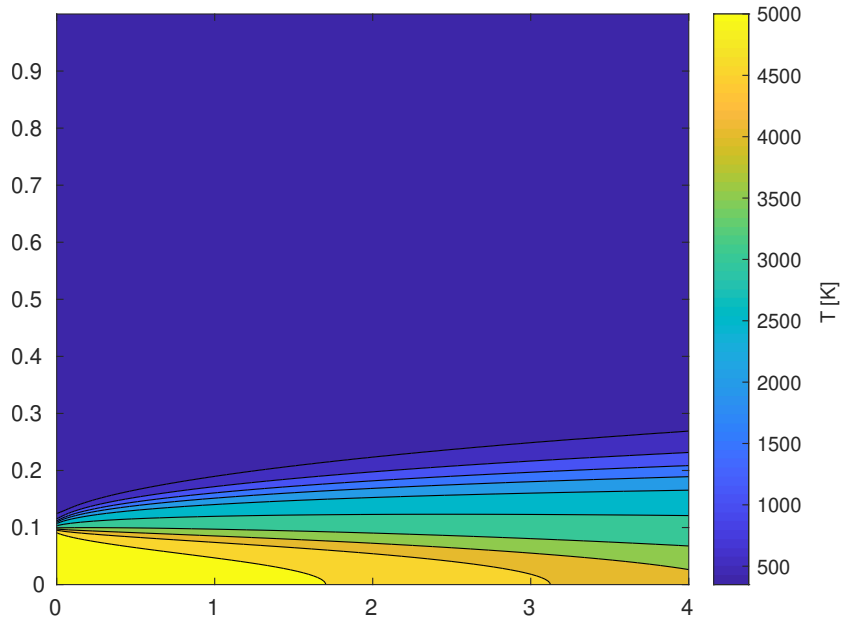

Mach can be as low as 10^{-4} in ICP!

Very low Mach simulations are ill-conditioned for numerical simulations...

Computational considerations: (very) low Mach

In high enthalpy flows, the **Mach can be very low**.

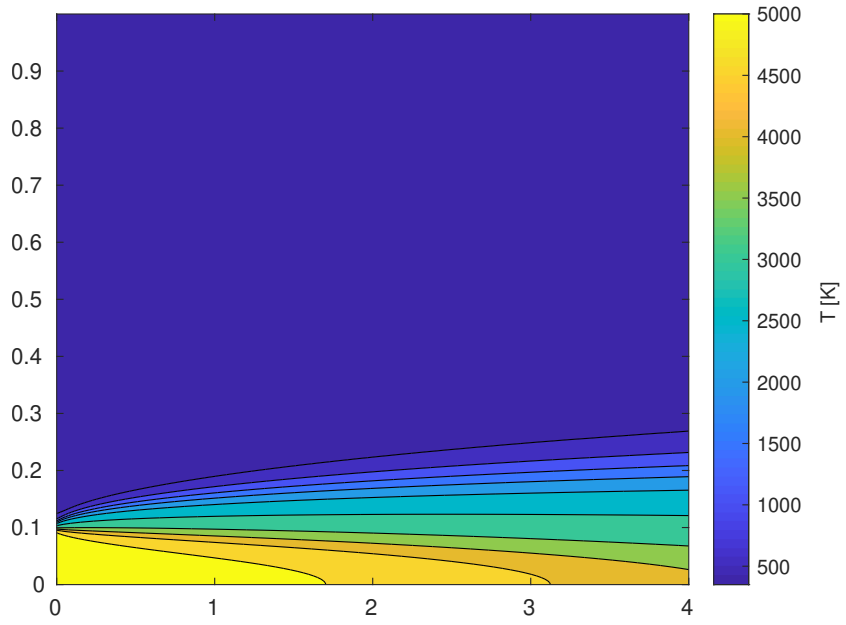

Mach can be as low as 10^{-4} in ICP!

Very low Mach simulations are ill-conditioned for numerical simulations...

Numerical flux: AUSM+up-As-cD (vector flux splitting).

$$F_{1/2} = \left(\dot{m}_{1/2} + w\dot{m}_p\right)\frac{1}{2}\left(\Psi_L + \Psi_R\right) - |\dot{m}_{1/2}|\frac{1}{2}\left(\Psi_L + \Psi_R\right) + P_{1/2}$$

Becomes **central at very low mach** and **upwind at mach > 1**.

Computational considerations: thermodynamic look-up table

Mutation++ is fast, but equilibrating a mixture remains expensive.

In high enthalpy flows, $p \simeq p_0$.

Idea: at p_0, compute the equilibria on a T grid, then interpolate the results.

N.B. this approach is often used in stellar plasmas.

Time preconditioning

Time preconditioning had to be implemented in the code in order to ease the convergence.

It is an alteration of the Jacobian matrix for rescaling the eigenvalues of the problem.

$$\begin{pmatrix} \partial_p \rho' & 0 & \partial_T \rho' \\ u\partial_p \rho' & \rho & u\partial_T \rho' \\ h_0 \partial_p \rho' - (1 - \rho \partial_p h) & \rho u & h_0 \partial_T \rho + \rho \partial_T h \end{pmatrix}$$

Result: Find a steady state with a classic Newton/GMRES solver without further modifications. Could be used for actual ICP.

Axisymmetric high-enthalpy jet

A hot jet (5250 K) is released in cold air (350 K).

Jet Velocity

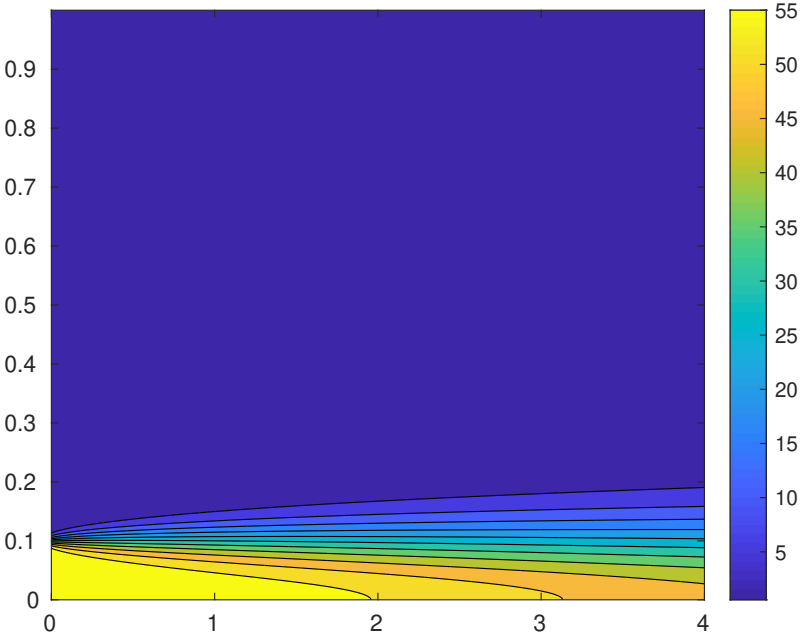

Jet Temperature

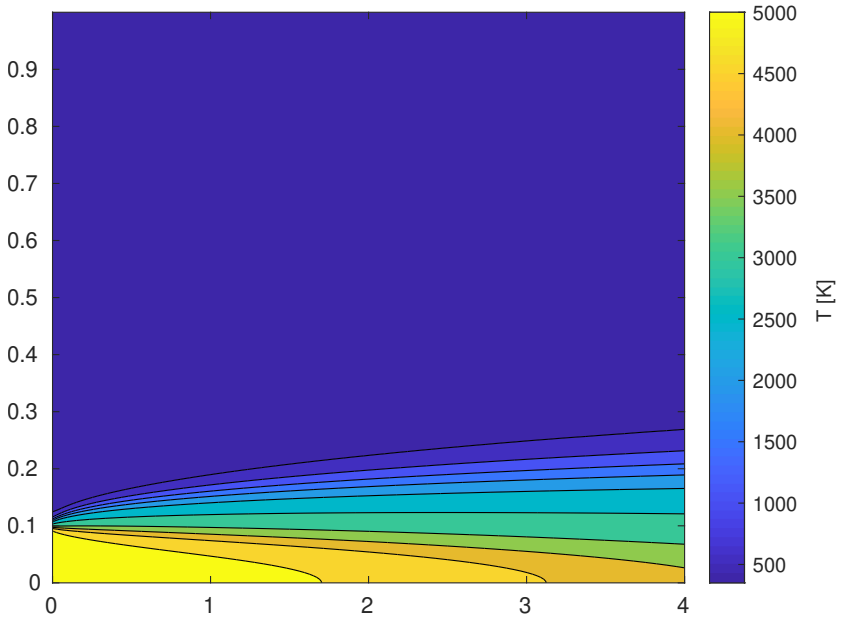

Axisymmetric high-enthalpy jet

A hot jet (5250 K) is released in cold air (350 K).

Jet Velocity

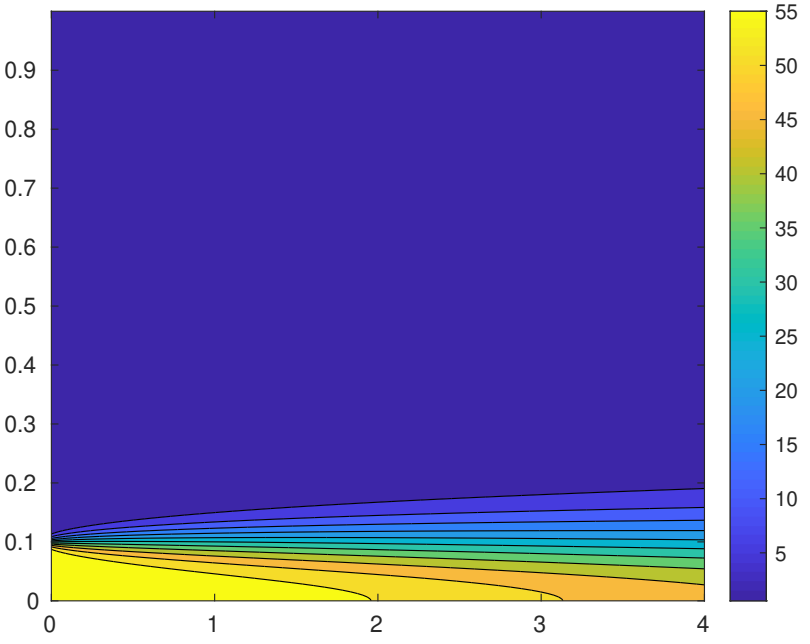

Jet Temperature

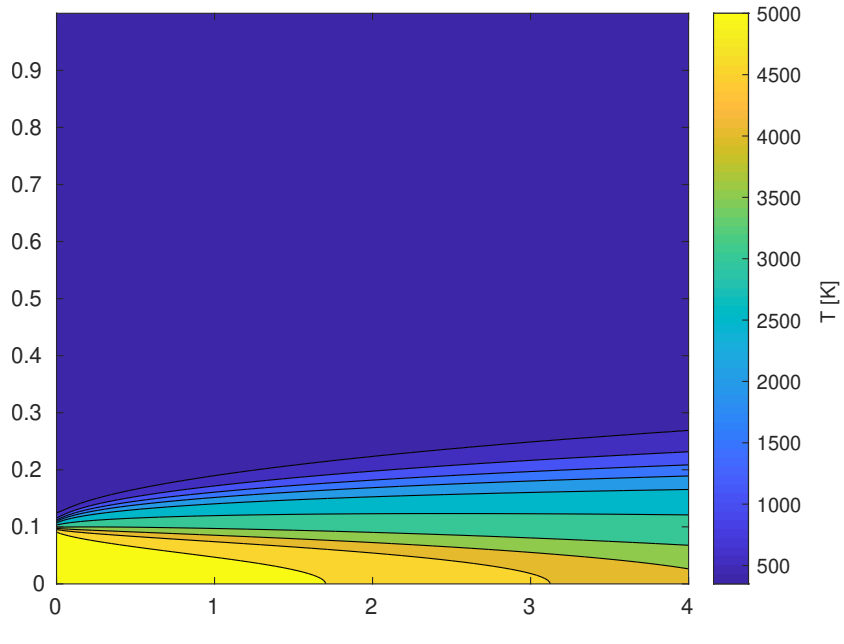

Low mach, chemistry effects, large temperature gradients, & test of Navier-Stokes

Jet results

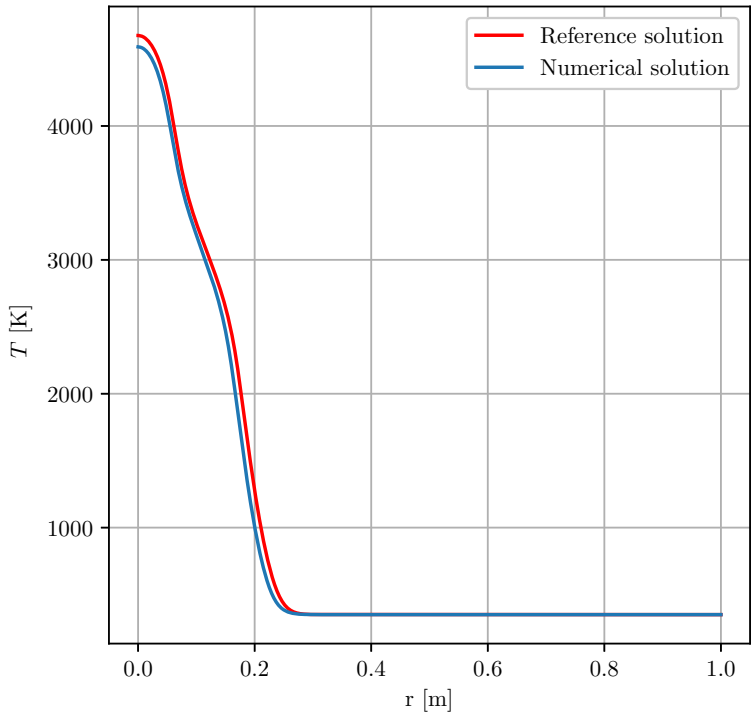

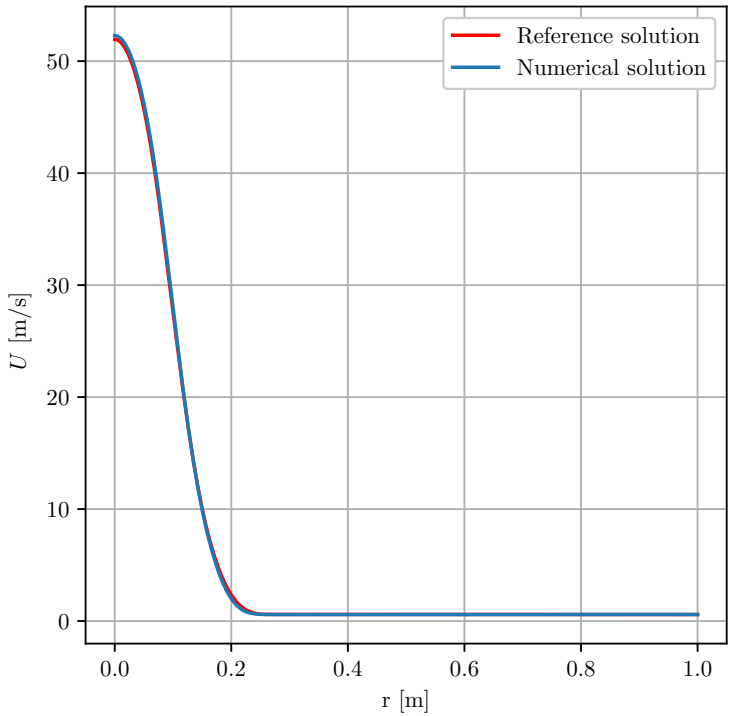

Disparity at the centerline between the expected and true temperature profiles.

Electromagnetism: the coil immersed in conducting air.

The equations to solve are derived from Maxwell's equations + simplifying hypothesis for axisymmetric ICP.

Electromagnetism: the coil immersed in conducting air.

The equations to solve are derived from Maxwell's equations + simplifying hypothesis for axisymmetric ICP.

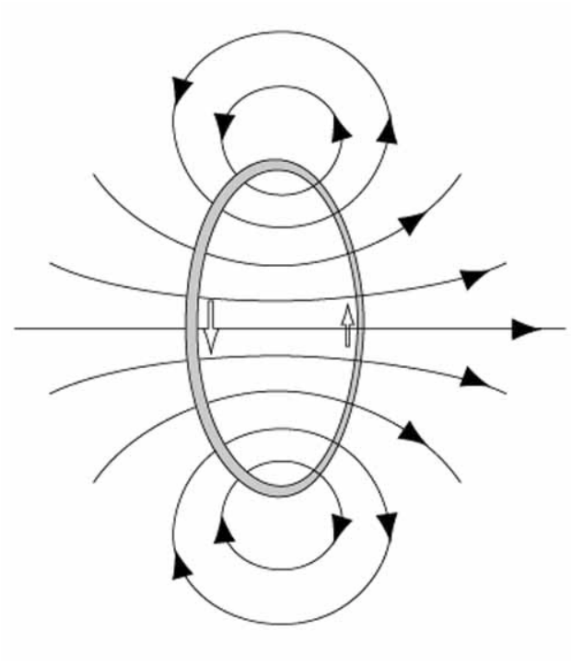

Electromagnetism: the coil immersed in conducting air.

The equations to solve are derived from Maxwell's equations + simplifying hypothesis for axisymmetric ICP.

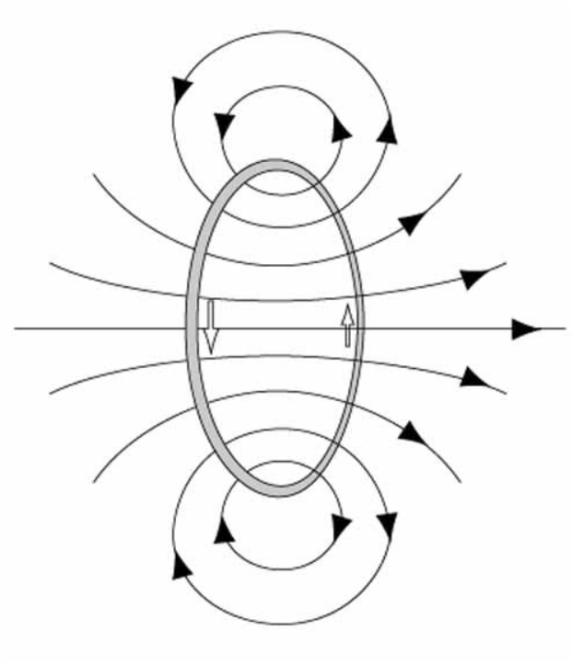

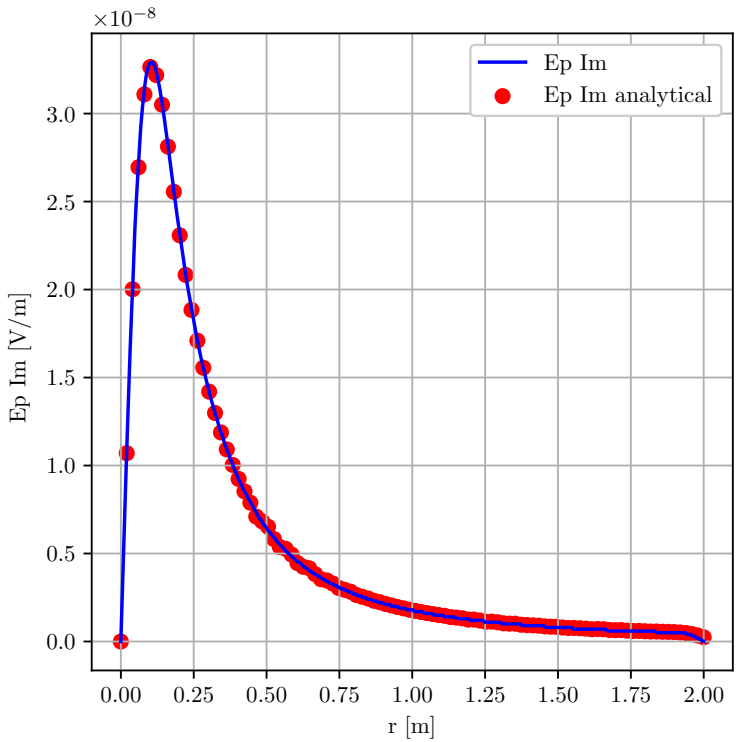

N.B.: Analytical solution involves elliptic integrals → python.

ICP system: a convergence study

Check the convergence of the method on the ICP equations using a manufactured solution u^*

ICP system: a convergence study

Check the convergence of the method on the ICP equations using a manufactured solution u^*

1. Plug u^* in

$$\nabla \cdot F(u) - S(u) = 0$$

ICP system: a convergence study

Check the convergence of the method on the ICP equations using a manufactured solution u^*

1. Plug u^* in

$$\nabla \cdot F(u) - S(u) = 0$$

2. The residual is the new source term:

$$\nabla \cdot F(u^*) - S(u^*) = S^*(u^*)$$

ICP system: a convergence study

Check the convergence of the method on the ICP equations using a manufactured solution u^*

1. Plug u^* in

$$\nabla \cdot F(u) - S(u) = 0$$

2. The residual is the new source term:

$$\nabla \cdot F(u^*) - S(u^*) = S^*(u^*)$$

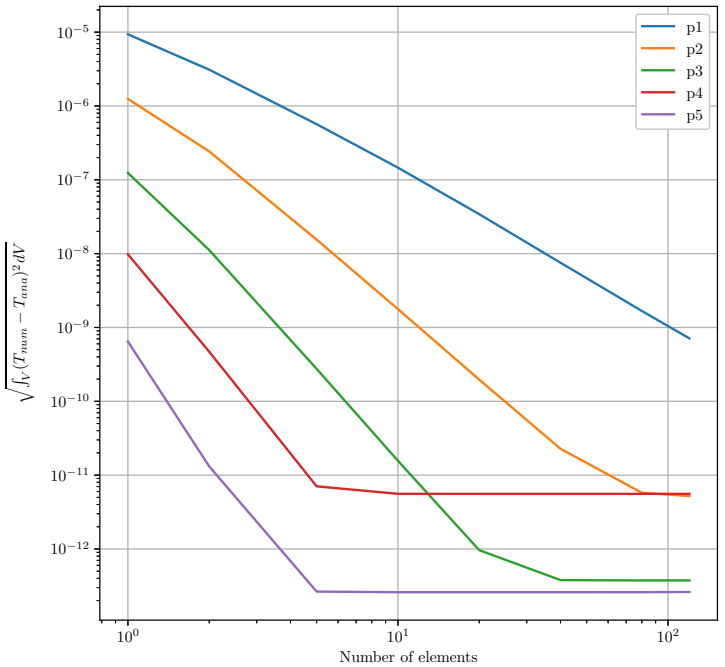

Rem: the manufactured solution is trigonometric.

Future considerations.

1. Simulations of ICP and verification with COOLFLuiD and litterature.
2. Multidomain simulations.
3. Time accurate simulations.
4. Code parallelization.
5. 3D modeling of plasma flows.

Back-ups

Derivation of electric field equation i

Maxwell's equation:

$$\begin{aligned} \nabla \cdot \mathbf{E} &= \frac{nq}{\epsilon_0}, \\ \nabla \cdot \mathbf{B} &= 0, \\ \nabla \times \mathbf{E} + \frac{\partial \mathbf{B}}{\partial t} &= 0, \\ \frac{1}{\mu_0} \nabla \times \mathbf{B} - \epsilon_0 \frac{\partial \mathbf{E}}{\partial t} &= \mathbf{j} + nq\mathbf{v}, \end{aligned} \tag{1}$$

Scalar and vector potential ϕ, $\mathbf{A}$:

$$\begin{aligned} \mathbf{B} &= \nabla \times \mathbf{A} \\ \mathbf{E} &= -\nabla \phi - \frac{\partial}{\partial t} \mathbf{A} \end{aligned} \tag{2}$$

Derivation of electric field equation ii

With the Lorentz gage,

$$\epsilon_0\mu_0\frac{\partial^2}{\partial t^2}\mathbf{A} = \nabla^2\mathbf{A} + \mu_0(\mathbf{j} + nq\mathbf{v})$$
$$\epsilon_0\mu_0\frac{\partial^2}{\partial t^2}\phi = \nabla^2\phi + \frac{nq}{\epsilon_0} \tag{3}$$

Split of electric field into electrostatic and induced parts:

$$\begin{aligned} E_I &= -\frac{\partial}{\partial t}\mathbf{A} \\ E_S &= -\frac{\partial\phi}{\partial z}\mathbf{e}_z - -\frac{\partial\phi}{\partial r}\mathbf{e}_r \end{aligned} \tag{4}$$

If no displacement current,

$$\nabla^2\mathbf{A} + \mu_0\mathbf{j} = 0 \tag{5}$$

Derivation of electric field equation iii

Ambipolar assumption ($j_z = j_r = 0$) and Ohm's law for unmagnetized plamsa $j_\theta = \sigma_e \mathbf{E}_I$.

Sinusoidal induction electric field:

$$\mathbf{E}_I = E_I \exp(i2\pi f t)\mathbf{e}_\theta \tag{6}$$

so that

$$\frac{\partial^2 E_I}{\partial z^2} + \frac{1}{r}\frac{\partial E_I}{\partial r}\left(r\frac{\partial E_I}{\partial r}\right) - \frac{E_I}{r^2} - i2\pi f \mu_0 \sigma_e E_I = i2\pi f \mu_0 I_C \sum_{i=1}^{nr} \delta(\mathbf{r} - \mathbf{r}_j) \tag{7}$$

Electric field produced by a coil:

$$\frac{\partial^2 E_C}{\partial z^2} + \frac{1}{r}\frac{\partial E_C}{\partial r}\left(r\frac{\partial E_I}{\partial r}\right) - \frac{E_C}{r^2} = i2\pi f \mu_0 I_C \sum_{i=1}^{nr} \delta(\mathbf{r} - \mathbf{r}_j) \tag{8}$$

Derivation of electric field equation iv

If one define E_P such that $E_I = E_C + E_P$, one has

$$\frac{\partial^2 E_P}{\partial z^2} + \frac{1}{r}\frac{\partial E_P}{\partial r}\left(r\frac{\partial E_P}{\partial r}\right) - \frac{E_P}{r^2} - i2\pi f\mu_0\sigma_e(E_C + E_P) = 0 \tag{9}$$

Note on ambipolar assumption: in the case of quasi-neutrality and no displacement current, the divergence of Maxwell-Ampere equation is

$$\nabla \cdot \mathbf{j} = 0. \tag{10}$$

The ambipolar assumption is compatible with it, but stronger in the sense that it forces the $\mathbf{j}$ components to be 0.

Manufactured solution

The manufactured solution is the following one:

$$\begin{aligned} T &= T_w + \Delta T \cos\left(\frac{r}{2R}\pi\right) \\ E_P &= E_0 \sin\left(\frac{r}{R}\pi\right) \end{aligned} \tag{11}$$

Chosen because T is max at center and electric field becomes 0 at both center and wall.

Time preconditioning

$$\begin{pmatrix} \partial_p \rho' & 0 & \partial_T \rho' \\ u\partial_p \rho' & 0 & u\partial_T \rho' \\ h_0 \partial_p \rho' - (1 - \rho \partial_p h) & \rho u & h_0 \partial_T \rho + \rho \partial_T h \end{pmatrix} \tag{12}$$

$$\begin{aligned} \partial_p \rho' &= \frac{1}{\epsilon c^2} \\ \partial_T \rho' &= \partial_T \rho \\ \epsilon &= \frac{M_p^2}{1 - \frac{M_p^2 \partial_T \rho' \alpha T}{\rho^2 \beta c_p - \alpha^2 \rho T}} \end{aligned} \tag{13}$$

Future considerations: Multi domain approach

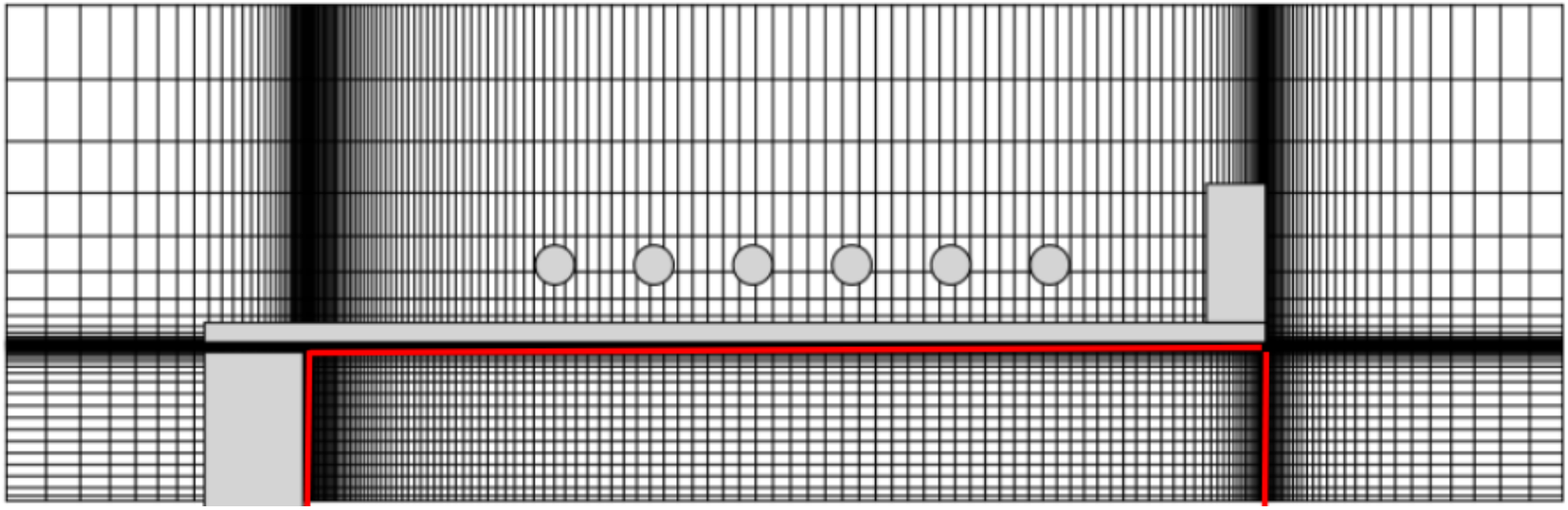

Rectangle inner region: full MHD equations.

Rectangle outer region: only electric field equation.